Low Temperature Physics/Fizika Nizkikh Temperatur, 2016, v. 42, No. 7, pp. 716–725

Luminescence of SiO_2 and GeO_2 crystals with rutile structure. Comparison with α-quartz crystals and relevant glasses

(Review Article)

A.N. Trukhin

Institute of Solid State Physics, University of Latvia, 8 Kengaraga Str., Riga LV-1063, Latvia
E-mail: truhins@cfi.lu.lv; truhins@latnet.lv

Received March 1, 2016, published online May 25, 2016

Luminescence properties of SiO_2 in different structural states are compared. Similar comparison is made for GeO_2. Rutile and α-quartz structures as well as glassy state of these materials are considered. Main results are that for α-quartz crystals the luminescence of self-trapped exciton is the general phenomenon that is absent in the crystal with rutile structure. In rutile structured SiO_2 (stishovite) and GeO_2 (argutite) the main luminescence is due to a host material defect existing in as-received (as-grown) samples. The defect luminescence possesses specific two bands, one of which has a slow decay (for SiO_2 in the blue and for GeO_2, in green range) and another, a fast ultraviolet (UV) band (4.75 eV in SiO_2 and at 3 eV in GeO_2). In silica and germania glasses, the luminescence of self-trapped exciton coexists with defect luminescence. The latter also contains two bands: one in the visible range and another in the UV range. The defect luminescence of glasses was studied in details during last 60–70 years and is ascribed to oxygen deficient defects. Analogous defect luminescence in the corresponding pure nonirradiated crystals with α-quartz structure is absent. Only irradiation of a α-quartz crystal by energetic electron beam, γ-rays and neutrons provides defect luminescence analogous to glasses and crystals with rutile structure. Therefore, in glassy state the structure containing tetrahedron motifs is responsible for existence of self-trapped excitons and defects in octahedral motifs are responsible for oxygen deficient defects.

PACS: **61.82.–d** Radiation effects on specific materials;
61.66.–f Structure of specific crystalline solids;
71.35.Aa Frenkel excitons and self-trapped excitons;
78.60.–b Other luminescence and radiative recombination.

Keywords: SiO_2, GeO_2, rutile, quartz, glasses, defects, self-trapped excitons, luminescence.

Contents

Introduction

Silicon dioxide could exist in many polymorph modifications. Polymorph modifications based on ability of silicon to sp^3 hybridization belong to a family of tetrahedron structured materials, silicon dioxide α-quartz (2.648 (α-quartz), 2.196 (amorphous) g·cm^{-3}) and that family could be accounted as mostly studied from fundamental science and from application point of view. Dense (4.28 g·cm^{-3}), octahedron structured, possessing rutile structure, polymorph

modification named stishovite is not well studied, however theoretic and experimental approaches of study are started now and first results are obtained [1–5].

Main element of structure of dense silicon dioxide — stishovite is based on another manner of silicon hybridization — d^2sp^3, providing octahedral surrounding of silicon with oxygen ions. Our interest lies in the study of changes of electronic states and point defects due to the transition from tetrahedron structured modification to octahedron structured one. We account that our knowledge of tetrahedron structured modifications of silicon dioxide is more detailed than that for octahedron structured modifications, then the last should be studied more. Optical methods are widely used for the examination of electron states and point defects, and we applied these methods for octahedral silicon and germanium dioxides.

Actually, it is little known about defects in stishovite. The role of a hydrogen in the form of an OH group was studied (see e.g. [6]), and it was found that IR spectra contain bands corresponding to OH. The influence of iron and aluminum impurity on OH IR absorption band intensity was studied. It was found that samples with or without iron possess the similar intensity of OH absorption, whereas aluminum impurity stimulates the intensity of OH IR absorption. Therefore it is possible to conclude that OH impurity mainly could be incorporated into defect structure, a host or an impurity.

In stishovite samples available for our investigation (synthetic monocrystals and Meteor Crater Arizona "natural" polycrystalline powder), there are two main luminescence bands: a blue one at about 3 eV and UV one at about 4.75 eV [1,3–5]. In addition, a quasimolecular luminescence center ascribed to the presence of carbon impurity was found [7]. Besides, OH groups in different concentration were found in both samples [7]. In Arizona stishovite the OH concentration is much higher. Although a center with quasi-molecular structure of luminescence band was also found in Arizona stishovite, there are no proofs of its connection with carbon impurity.

Good analogy with polymorphism of silicon dioxide is observed for germanium dioxide. The GeO_2 can exist in hexagonal structure. Hexagonal GeO_2 has the same structure as quartz. The hexagonal (d = 4.29 g/cm^3) form of germanium dioxide is more soluble than the rutile one (d = = 6.27 g/cm^3). Both silicon dioxide and germanium dioxide are known in amorphous or glassy states. So, the studies of these different materials with similar method give good opportunity for the comparison and modeling of different structure influence on the material properties.

Experimental details

The stishovite single-crystals were grown under hydrothermal conditions by methods published in [8,9]. The samples of investigation were small optically transparent single-crystals with the dimensions about (0.2–0.4)×0.6×0.9 mm. The samples were kept on a copper holders covered with an indium layer possessing a hole, where the samples were pressed into avoiding slits let light through. The excitation was made from one side of the holder and detection from another, thus excluding possible luminescence of contamination on the surface of the holder. A pure silicon dioxide quartz crystal and a pure silica glass sample were used for comparison.

Tetragonal GeO_2 crystals were grown from the melt of germanium dioxide powder mixed with sodium bicarbonate by the "top-seed" method [10]. That mixture is cooled down below the fusion temperature of 1050 °C. In such a way the transition of the hexagonal phase to the tetragonal one is achieved. The crystals were grown on a seed rod introduced to the liquid surface. The remaining fusion after cooling was in a glassy state. The samples were well shaped crystals with dimensions of about 4×1×1 mm. A germanium dioxide quartz sample was grown on quartz plate [11].

The optical absorption was measured with Hamamatsu mini spectrometer and optical fiber using a deuterium discharge lamp as light source. Initially, the spectrum of light source was measured through an empty hole with the dimensions that approximately fit the samples dimensions. Then the spectrum of light passed the sample was measured. The optical fiber was put directly (or) on the hole or on the sample at a sample holder. The absorption spectra in vacuum ultraviolet (VUV) region were measured using the 0.5 m Seya-Namioka vacuum monochromator. The spectra of transmittance and absorbance were subsequently calculated in relative units. The measured spectrum was sewed with this measured in VUV range.

The KrF, ArF and F_2 lasers (model PSX-100, made by Neweks, Estonia) as well as an x-ray tube were used as luminescence excitation sources. The F_2 laser (157 nm) has a pulse energy of about 0.5 mJ with a duration of 5 ns, while power of the KrF (248 nm) and ArF lasers (193 nm) was 7 times higher. The light of the F_2 laser was passed through a copper tube with flow of nitrogen. The light of the KrF and ArF lasers was put on the sample through atmospheric air. The excitation laser was located on 1-m distance from the sample. The beam size of the laser was 2×2 mm. The crystalline silicon dioxide α-quartz with low level of luminescence was used as a window to pass through the light of the excitation lasers. The photoluminescence (PL) intensity of the studied samples depended linearly on the excitation intensity; therefore, a single photon excitation regime was used. The monitoring of excitation intensity was realized via LiF crystal plates of different thickness, the attenuation degree of which was determined using a power-meter.

The x-ray tube was with W anticathode working in the regime of 50 kV and 20 mA. Two cryostats were used. The first cryostat maintains temperature in the range 60–400 K,

the lowest temperature was achieved by pumping of liquid nitrogen from the cryostat. Some measurements were realized with the use of a helium refrigerator. The temperature range in this case was 16–300 K. Luminescence detection was realized through a grating monochromator MCD-1 with a photomultiplier (PM) tube H6780–04 with 50 Ohm resistive load. The optical filters were employed for cutting laser light in the line for luminescence detection. An oscilloscope (Textronic TDS 2022B) was exploited for decay curve registration. Each curve was averaged for 128 pulses. The time resolved spectra were measured by registration of the decay curve for each point of the PL spectrum in two time ranges — one in ns range another in μs range. The measured curves are presented in figures as-received, therefore, they reflect the level of errors. The discharge of excimer laser provides strong stray current in the measurement circuit, which distorts signal for short time range.

The x-ray excited spectra were measured in the photon counting regime using a PM FEU-106. The PL decay kinetics of long duration and low intensity (unable to be measured in current regime) was recorded with the use of a photon pulse time analyzer. The spectra in IR range where measured with FTIR spectrometer Bruker Equinox 55.

Results and discussion

Luminescence of stishovite single crystal

The x ray excited luminescence spectra are presented in Fig. 1. It should be underlined that the x-ray excitation was performed only after PL measurements were done. The same two bands in the blue (~ 3.1 eV) and UV (~ 4.75 eV) parts of spectra are observed in the x-ray excited spectrum. Nothing was changed in PL spectra before and after x-ray excitation, that showing little influence of x-ray irradiation on the luminescence center. Additional irradiation with an electron beam was performed as well. According to Fig. 1, the latter strongly diminishes x-ray excited luminescence [12].

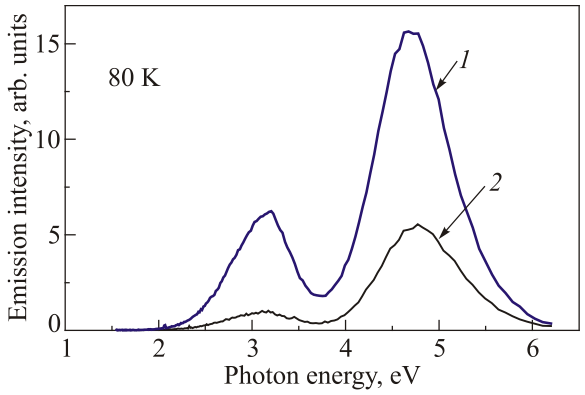

Fig. 1. The x-ray excited spectra of a stishovite single crystal measured before and after irradiation with an electron cannon pulses (270 kV, 200 A, 10 ns duration of pulse): nonirradiated (*1*), irradiated (*2*).

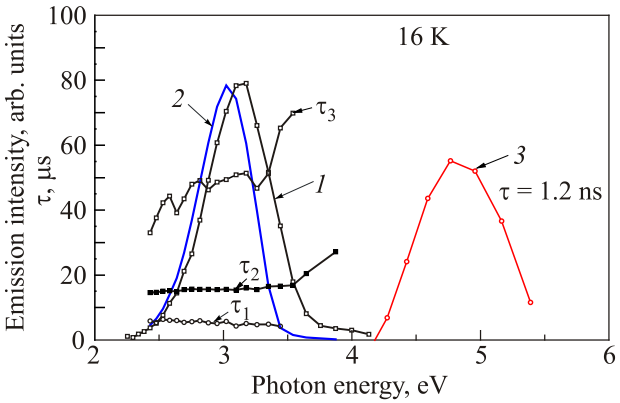

Fig. 2. (Color online) Time resolved PL spectra of a stishovite single crystal excited by the ArF laser at 16 K. A fast component also takes place causing the shifting of PL spectrum towards high energies. Fast decay for UV band is with τ ~ 1.2 ns. Integral of kinetics curves within interval 0–1 μs (*1*), integral within interval 1–100 μs (*2*), integral within interval 0–30 ns (*3*), τ_1, τ_2, τ_3 — approximation with exponents of different parts of the blue band decay curves.

So, electron irradiation does not create novel luminescence centers in the sample under investigation and, tentatively, even destroys the existing.

Time-resolved PL spectra of a stishovite single crystal under ArF laser excitation are presented in Fig. 2. Blue band decay comprises several components in the range 1–100 μs, while the main component is with the time constant about 18 μs. The main decay component for the UV band is about 1 ns.

The temperature dependences of the intensity of two x-ray excited luminescence bands measured by a photon counting method are presented in Fig. 3.

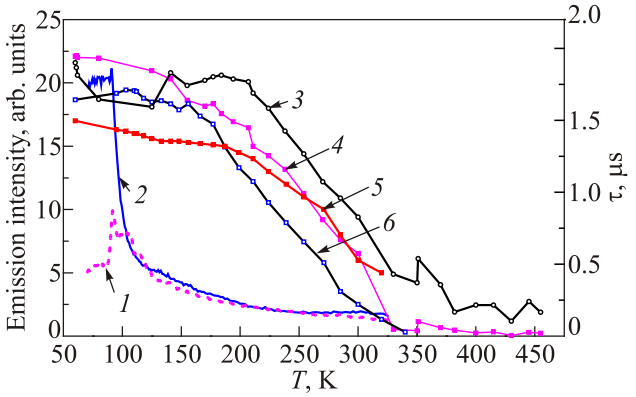

Fig. 3. (Color online) Temperature dependences of the intensities of x-ray excited blue (*1*) and UV bands (*2*) with E_{act} ~ 0.025 eV for both bands, as well as of time resolved PL intensities (obtained by integrating the decay curves) and decay time constants of principal part of decay excited by the ArF laser. The energies of thermal quenching are presented: blue, τ(μs), E_{act} = 0.21 eV (*3*), blue, intensity, E_{act} = 0.22 eV (*4*), UV, τ(ns), E_{act} = 0.11 eV (*5*), UV, intensity, E_{act} = 0.1 eV (*6*).

These data are compared with those for the intensity of blue and UV time resolved PL as well as temperature dependences of time constants for both bands in a stishovite single crystal excited with the ArF laser. A noticeable effect was observed: significant fall down in intensity of x-ray excited luminescence at 100 K does not correspond to the changes in thermal dependences of PL parameters. The parameters of thermal dependences were determined according to Mott's law:

$$I(T) = I_0\left(1 + f\cdot\tau_0\exp\left(-E_a / kT\right)\right)^{-1}, \qquad (1)$$

where I is the intensity at a certain temperature and I_0 is intensity of non-quenched transitions. For the case of x-ray excitation, the average value of activation energy is E_a = = (0.03±0.01) eV and frequency factors equal to f(UV) = = 10^{11} s^{-1}, f(blue) = 10^7 s^{-1}, while for the case of PL, E_a = = (0.15±0.05) eV, f(UV) = 10^{12} s^{-1}, f(blue) = 10^9 s^{-1} [12]. So the processes of thermal quenching are different for these kinds of excitation.

In Fig. 4 the photoluminescence excitation (PLE) spectrum for the blue PL band is compared with the absorption spectrum [7]. The PLE of UV band was not measured yet due to emission low intensity. The PLE of the blue band is detected in the range 5–11 eV. It could be only assumed that the PLE of the UV band has similar behavior.

In Fig. 5 the PL spectra of a synthetic stishovite single crystal and a shock-wave created stishovite powder from a large meteorite striking the earth are compared. It is seen that there are differences in the position of the blue band and NIR luminescence. The positions of NIR PL lines of the Arizona natural sample differ from those for the single crystal and are situated at 689 nm (1.789 eV), 694 nm (1.785 eV) and at 706 nm (1.754 eV) (Fig. 5.)

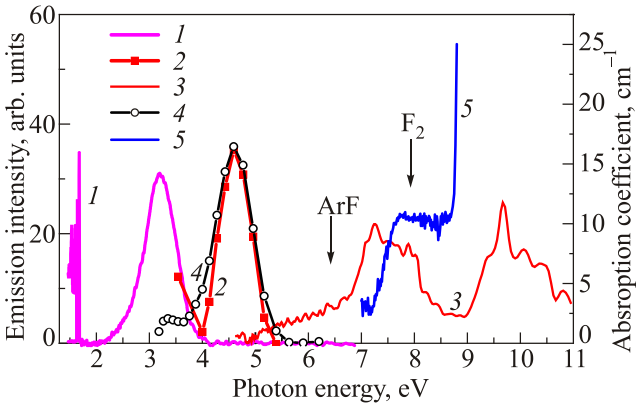

Fig. 4. (Color online) Photoluminescence (PL), photoluminescence excitation (PLE) of the blue band and the absorption spectra for a synthetic stishovite single crystal. Open circles and filled square represent time resolved spectra. PL line is measured with CCD of a Hamamatsu minispectrometer. Intensity of PLE is detected by a photon counting method. T = 290 K. F_2 excited PL (*1*), F_2 excited fast (~ ns) PL (*2*), PLE of the band at 3 eV (*3*), ArF excited fast (~ ns) PL (*4*), absorption spectrum (*5*).

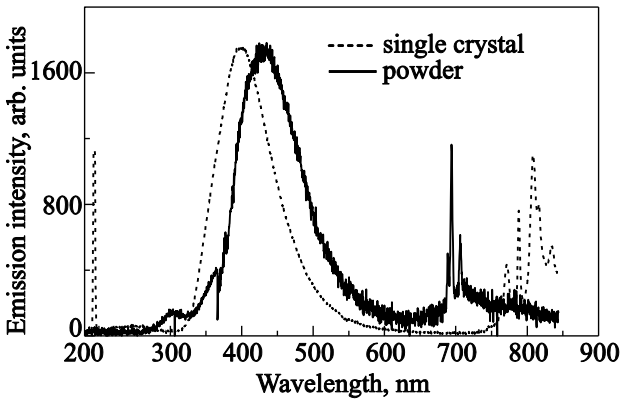

Fig. 5. PL spectra of a synthetic stishovite single crystal and natural shock-created stishovite powder from Meteor Crater, Arizona. The used optical filters allow avoiding a direct hit of excitation light from the ArF laser (193 nm).

The part of PL spectra in the NIR range for the monocrystalline stishovite is presented in Fig. 6. The line at 771 nm is absent at 80 K, and, thus, it may be ascribed to an anti-stokes transition, whereas the sharp line at 787 nm may be a zero phonon line. Its intensity increases with cooling.

IR spectra of the samples under comparison are presented in Fig. 7. The intrinsic IR spectra are well corresponding mutually. Also the bands in the range of OH absorption are sufficiently similar, whereas the bands of Meteor Crater stishovite are broader and more intensive. The concentration of OH groups in Meteor Crater stishovite therefore is much higher.

We have observed luminescence in as-grown single crystals of dense silicon dioxide polymorph modification — stishovite. So, the luminescence centers exist in nonirradiated samples. The luminescence possesses two main bands [1,3–5,7,12]. The blue band has a time constant about 17 μs in the range 16–200 K and, because of long duration, (it) is due to forbidden transitions in an intracenter process. The UV band is fast with τ about 1.2 ns and is due to allowed transitions. Both bands can be also excit-

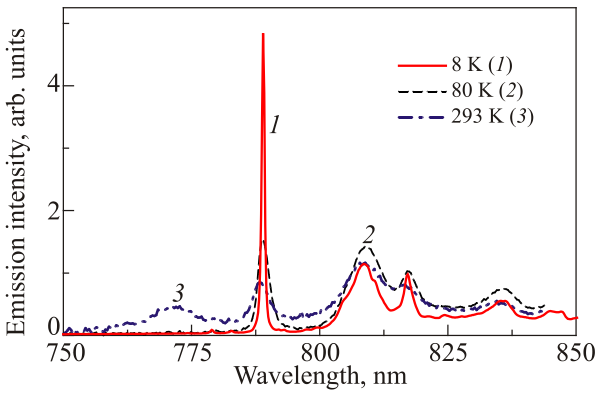

Fig. 6. (Color online) Near infrared luminescence of stishovite excited with ArF laser.

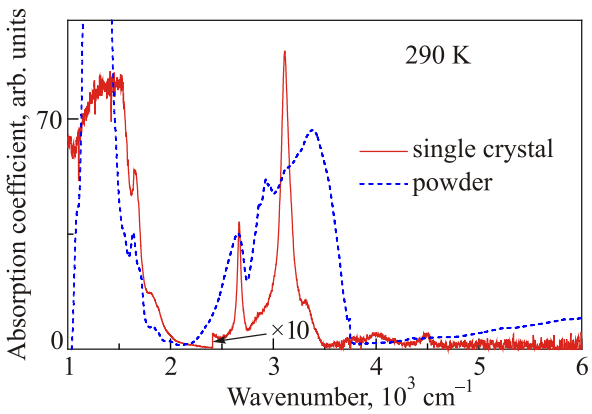

Fig. 7. (Color online) IR absorption spectra of a synthetic single crystal and a natural stishovite powder (shock-wave-produced). The range above 2000 cm^{-1} matches to OH absorption.

ed via the recombination process and undergo thermal quenching in the same temperature range. Therefore, the bands can be ascribed to the same center.

The samples possess OH groups detected via IR absorption spectra measurements (see Fig. 7). As mentioned, OH groups in stishovite could be mainly connected with defects in general [6] and, in our particular case, with the defect serving as a luminescence center. Interaction of a PL center with an OH group, causing the creation of a complex PL center–OH group, can explain the peculiarities in decay kinetics. Laser irradiation provokes photolytic reaction in this complex, thus changing bonding and distances. Normally, an OH group that interacting with a luminescence center provides luminescence quenching effect in the case of many centers (see e.g. [13]). Removal of OH group due to absorption of a photon activates the luminescence center [13]. Different distances between a luminescence center and a separated OH group could modulate population on the excited state, variating decay kinetics. Indeed, on the main decay kinetics curve for blue luminescence besides the well-defined exponent with decay time of 17 μs, we have some growth in time of range of μs units that is far away from an excitation pulse. The nearest OH group could affect life time on the excited state.

The effect of the strong fall down (Fig. 3) at 100 K in x-ray excited luminescence and lack of such decrease in PL at that temperature could be explained by differences of OH interaction with the center performing radiation transitions in intracenter process and recombination process. X-ray luminescence appears in recombination process mainly. Probably, the OH groups are participating in charge trapping, providing competitive trapping of charge and thus diminishing luminescence intensity. Perhaps, the value of 100 K is a threshold for the OH group motion in the studied material. At temperatures above 100 K OH easy comes back to the center and quenches the luminescence. The interaction of interstitials with luminescence centers explains a low quantum yield of photoexcitation and a high energetic yield of the excitation with ionizing radiation — x rays and an electron beam. This leads to the changing of lifetime and quenching of luminescence by transferring energy of an excited luminescence center to a molecular defect. Deactivating changes quantum yield and monitoring of the transition probabilities. ionizing irradiation could remove the molecular defect; in such case luminescence becomes bright and most of the absorbed energy is irradiated. At lower temperatures the detached molecular defect could be trapped in lattice far away from the luminescence center. Above 100 K the molecular defect could be released from traps by vibration and returns back. In such conditions the energetic yield of UV luminescence under ionizing radiation significantly drops down at higher temperatures.

The influence of the molecular defect on decay of blue luminescence could be explained by assumption that the luminescence center in excited triplet state repulses the molecular defect on a distance and if this triplet state is occupied, the influence of the molecular defect is diminished and the yield of blue luminescence is high enough.

Now, we compare luminescence of stishovite with oxygen deficient centers (ODCs) of luminescence of silica glasses (details will be presented below). However ODCs properties are different in dry silica and wet silica. Therefore is not one to one correspondence between ODC in dry silica glass and stishovite because of OH groups presence in the latter. On the other hand, if we deal with OH-containing silica glass, there is significant difference in OH groups' incorporation into silica glass and crystals. In crystals, an OH group occurs in form of an interstitial, in silica glass OH is mainly incorporated in the glass network as Si–O–H. Therefore, there is no possibility for one to one comparison of the studied luminescence centers in OH-containing stishovite and wet silica glass.

The performed investigations show that the luminescence center in stishovite, dense polymorph modification of silicon dioxide, exists in as-grown single crystals. The luminescence spectrum consists of two bands, a slow blue one at (3±0.2) eV with main life time of 17 μs and a fast UV band at (4.7±0.1) eV with life time of 1.2 ns for thermally non-quenched intracenter transitions. A correlation is found between the presence of OH group in stishovite crystal and peculiarities in decay kinetics of the blue luminescence. The observed growth kinetics is explained by motion of nearest OH group, which affect emitting properties of the center. The observed luminescence center in stishovite is very similar to oxygen deficient center of luminescence in silica glass and damaging radiation induced luminescence center of α-quartz crystal.

Comparison of stishovite luminescence with that of irradiated SiO_2*-quartz*

In the Fig. 8 the x-ray excited emission spectrum of stishovite is compared with the cathodoluminescence spectrum of pure α-quartz [14].

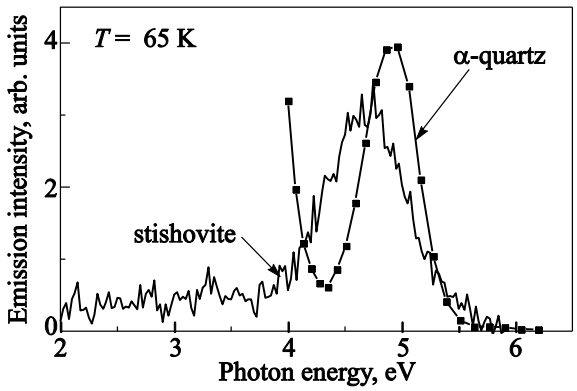

Fig. 8. (Color online) X-ray excited luminescence spectrum of dense silicon dioxide crystal-stishovite (line) and cathodoluminescence of pure silicon dioxide α-quartz crystal at 65 K. X-ray parameters — *W* anticathode, 50 kV, 20 mA. Electron beam parameters 10 kV, 1 μA, defocused. Strong growth of the intensity at 4 eV in α-quartz is related to the self-trapped exciton luminescence [4].

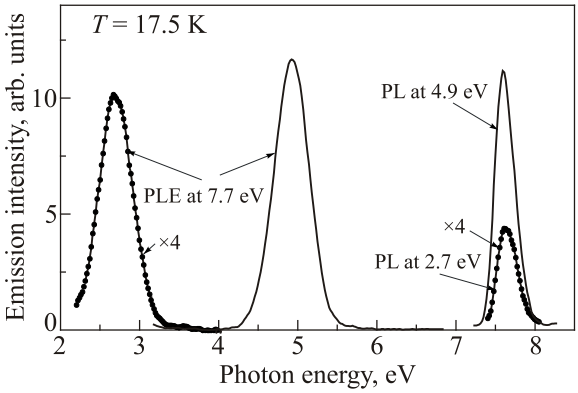

Fig. 10. The photoluminescence and it excitation spectra of γ-irradiated sample of pure crystalline α-quartz at T = 17.5 K [16]. It consists of two emission bands peaked at ~ 2.7 and ~ 4.9 eV, both excited at 7.6 eV.

The UV luminescence was exhibited in α-quartz crystal only after dense electron beam irradiation at temperatures below 70 K (Fig. 9) and induced centers were not stable — they could be annealed by heating to room temperatures [15]. Cathodoluminescence intensity grows from very low initial state in Fig. 9 to some saturation state. This saturation state could be explained by a back-reacting of detached neutral oxygen ions with oxygen vacancies.

Destructive neutron and gamma irradiations are able to make this center stable at room temperature. γ-irradiation gives induced luminescence center in α-quartz (see for example [16]), Fig. 10, where a UV band at 4.9 eV and a blue band at 2.7 eV are observed. The decay time constant of UV band is 1 ns and that for blue band is 3.6 ns at 17.5 K under excitation with 7.6 eV photons of synchrotron light source [17]. While there is some correspondence between the decay of ODCs UV band in silica and gamma irradiated α-quartz, there is no correlation for the blue band. The induced blue band in α-quartz is too fast. In [4], similarity is presumed between centers in both polymorph modifications — stishovite and irradiated α-quartz. "Soft" x-ray irradiation is not able to create this center in α-quartz. In the latter, only the dense electron beam irradiation can create such center, which is stable only at low temperatures. In pure virgin α-quartz crystal under x-ray irradiation only luminescence of the self-trapped exciton could be observed (see below).

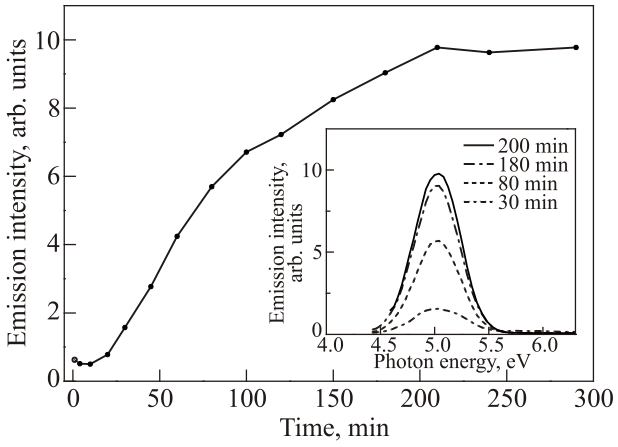

Fig. 9. Cathodoluminescence dose dependence and spectra (insert) of pure crystalline quartz at different irradiation times [15]. T = 10 K. Electron beam parameters 10 kV, 1 μA.

Luminescence of oxygen deficient centers in pure silica glass

Blue and UV luminescence initially was observed in as-received oxygen deficient silica glass (now we will discuss properties of extremely pure silica glass samples). The study of luminescence mechanisms in pure, hydroxyl-free non-irradiated silica undertaken in the last half century revealed the importance of ODC**s** for these processes [18,19]. There are two main ODC**s** types: ODC(I) and ODC(II). Both are characterized with a blue luminescence band centered at 2.7 eV and a UV band at 4.4 eV. For ODCs(II) both bands can be excited by 5 eV and 7 eV photons, whereas for ODCs(I) — by 7.7 eV photons only. A rather reasoned structural model for the ODC(II) is a twofold coordinated silicon, containing a lone pair of valence electrons in ground state [18,19]. Electron transition accompanied by 5 eV photon absorption corresponds to a singlet-to-singlet excitation followed by respective allowed $^1S_1$–$^1S_0$ radiative transition yielding UV luminescence band, with life time τ = 4.5 ns [19]. Transition to a triplet excited state is associated with a weak absorption band centered at 3.3 eV and causes blue $^3T_1$–$^1S_0$ luminescence with τ = 10.3 ms. The triplet state is excited mainly at the expense of a conversion from the excited singlet state. The distinctive feature of ODCs(I) is UV luminescence, with life time 2 ns [20,21]

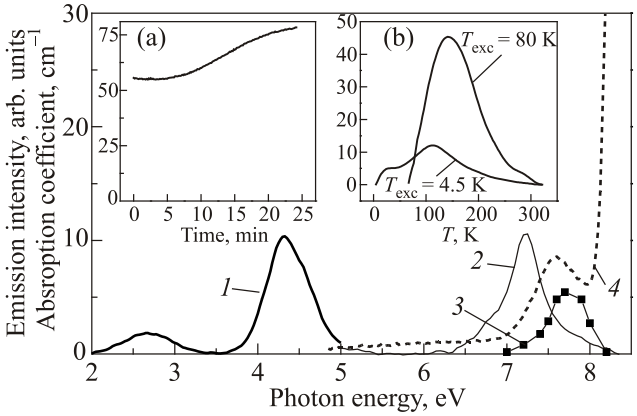

Fig. 11. Optical properties of silica glass (KC-4B). Photoluminescence (PL) excited at 7.7 eV (*1*) and photoluminescence excitation (PLE) detected at 4.4 eV spectra at 80 K (*2*), excitation spectrum of the peak at 100 K of thermally stimulated luminescence (TSL) (*3*), absorption spectrum (*4*). Insert (a) contains the time dependence of PL intensity at 4.4 eV under continuous excitation by 7.7 eV photons. Insert (b) the TSL curves for two temperatures of excitation, 4.5 and 80 K.

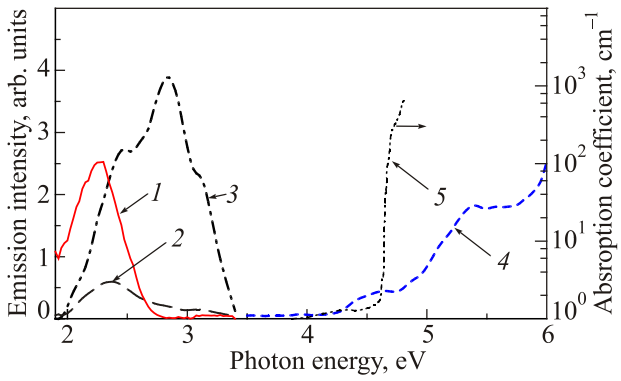

Fig. 12. (Color online) GeO_2-rutile-like crystal photoluminescence. PL, excitation by N_2 laser (337 nm), T = 80 K (*1*); PL excited at 5 eV, T = 290 K (*2*); PL excited at 5 eV, T = 80 K (*3*); PLE of the band at 3 eV, T = 80 K (*4*), intrinsic absorption threshold (77 K) [23] (*5*).

and excitation there of recombination luminescence [22]. In Fig. 11 the data for a pure silica glass with relatively high concentration of ODC(I) are presented. Here the band of ODC(II) is practically hardly observable. The PLE band is shifted to low energy with respect to the absorption band at 7.6 eV, however excitation of thermally stimulated luminescence (TSL) is shifted to the higher energy. So these shifts are due to ionization of the center leading to diminishing of steady state luminescence yield and increase of light sum storage on some traps.

Luminescence of rutile-structured GeO_2 *crystal. Comparison with glassy* GeO_2

Luminescence investigation of rutile-structured GeO_2 and comparison of that with glassy GeO_2 was done similarly to analogous procedure related to rutile-structured SiO_2 described in previous chapters. Saying forward, the obtained conclusions for the case of GeO_2 studies in general are similar to that for the case of SiO_2. However there are differences in the details related to difference in material preparation. While rutile-structured SiO_2 was obtained in extreme conditions of high pressure, the rutile-structured GeO_2 was obtained in relatively simple way. Tetragonal or rutile GeO_2 crystals were grown from the melt of germanium dioxide powder mixed with sodium bicarbonate by "top-seed" method [10]. That mixture is lowering of the fusion temperature down to 1050 °C. In such a way the transition of the hexagonal phase to tetragonal one is achieved. The crystals were grown on seed rod inserted into liquid surface. The remaining fusion after cooling was in glassy state. The samples were well shaped crystals with dimensions about 4×1×1 mm. So, these samples are much bigger than that of stishovite. However also in this case small dimensions of samples reduced ability to measure optical absorption and reflection spectra, therefore mainly luminescence measurements were performed. The samples of glassy germanium oxide also were studied for comparison. These were sample taken from glassy part of the same fusion, where crystals were grown.

Optical properties of GeO_2-rutile crystal are presented in Fig. 12. The intrinsic absorption threshold is situated at about 4.6 eV [23]. Its position is shifted to low energy side with respect to quartz-GeO_2 where it is situated at about 6 eV [24]. In this respect rutile GeO_2 differs from rutile SiO_2 with absorption threshold at 8.75 eV, which is higher than in quartz-SiO_2 (8.5 eV at 293 K, [3]).

The sample of ritile-GeO_2 possesses two main PL bands at about 2.3 eV and at 3 eV. Corresponding luminescence decay kinetics are presented in Fig. 13. The decay of green luminescence is slow with time constant about 190 μs. The decay of PL at 3 eV is fast (see Fig. 13 insert) and repeats an excitation pulse of the KrF laser (the corresponding decay time constant could be about 1 ns).

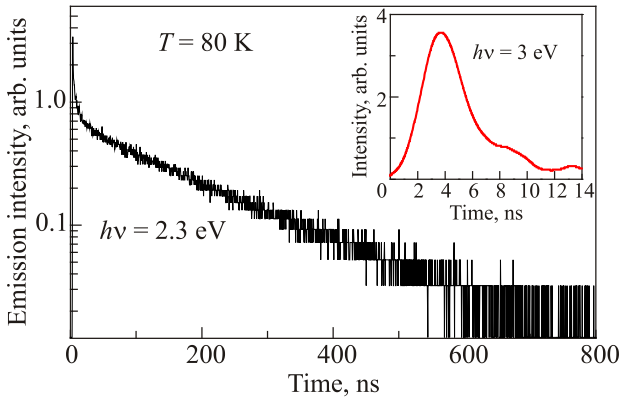

Fig. 13. GeO_2 rutile-like crystal, KrF laser excitation, basic panel — 2.3 eV luminescence band decay kinetics, insertion — 3 eV luminescence band decay kinetics, T = 60 K.

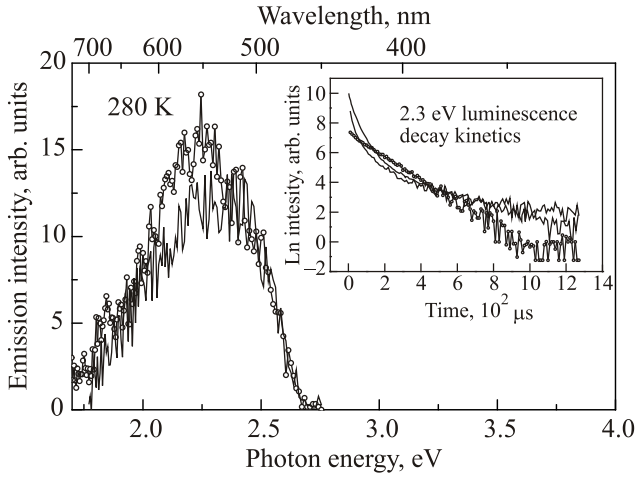

Fig. 14. Comparison of luminescence in crystalline (rutile) and glassy state of GeO_2 prepared under similar conditions as well as in $Na_2O{\cdot}3GeO_2$ oxygen deficient glass (the kinetics curves in the insertion are not specified because they are very similar to glass prepared together with the rutile GeO_2 crystal) [22]. Circles — rutile-like crystal, lines — glasses.

It should be mentioned that rutile-GeO_2 prepared from the melt mixed with sodium bicarbonate may be contaminated with presence of sodium and the luminescence center is modified by sodium. Luminescence of rutile germania crystal, grown from fusion in the presence of sodium bicarbonate as catalyst, and sodium germanate glasses, obtained from the same fusion with cooling, is practically identical Fig. 14, [22]. Difference is observed in decay kinetics. It is exponential in the crystal case and nonexponential in the glass case. Luminescence is ascribed to triplet-singlet transition of ODCs modified with sodium in both cases of crystal and glass. So, ODCs luminescence was found in germania crystal with rutile structure. The band at 3 eV with fast decay is ascribed to singlet-singlet transitions in ODCs — like defect with nearest sodium ion.

Germania glass free from sodium possesses singlet-singlet ODCs luminescence band at 4.1 eV, which is two-fold coordinated germanium without sodium modification [25]. A question stands, if germania crystal with rutile structure possesses analogous singlet-singlet luminescence unperturbed with sodium defect. Such a band was found under ArF laser excitation in such crystal [26] and its spectra are presented in Fig. 15. Certainly, a laser excitation photon falls down deeply in the intrinsic absorption range and it also provides recombination luminescence with slow decay [26].

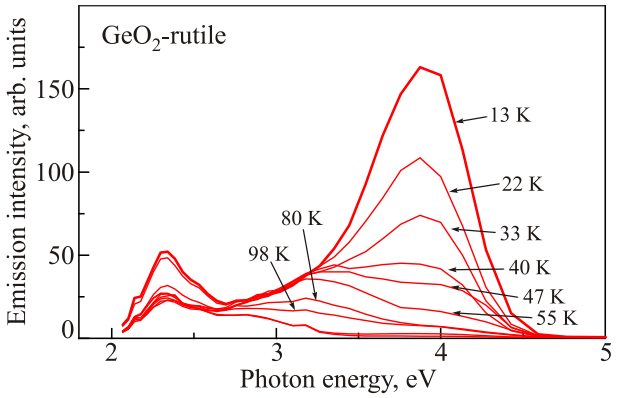

Fig. 15. GeO_2 rutile-like crystal, ArF laser excitation, PL spectra at different temperatures, [26].

Luminescence of α-quartz-structured SiO_2 *and* GeO_2 *crystals. Self-trapped exciton*

In nonirradiated quartz crystals, both SiO_2 and GeO_2 luminescence similar to rutile-structured SiO_2 and GeO_2 were not observed. As it is presented above, in a quartz crystal irradiation provides luminescence similar to rutile-structured crystal. Also in nonirradiated α-quartz crystals no luminescence similar to oxygen deficient silica glass was observed. On the other hand, both SiO_2 and GeO_2 quartz crystals provide very intensive luminescence excitable only in the range of intrinsic absorption. In Fig. 16 the spectral characteristics of quartz crystal SiO_2 and GeO_2 as well as SiO_2–Ge are presented. In quartz GeO_2 as well as SiO_2–Ge the photoluminescence appeared with high (~ 0.4) quantum yield. In quartz SiO_2 the photoluminescence has small yield (~ 0.05) whereas under x ray its energetic yield reaches the level of about 20% of absorbed energy [22].

The luminescence band Stokes shift is large. The presented data for the case of quartz crystal SiO_2–Ge underline the difference from glassy SiO_2–Ge, where luminescence is due to the twofold-coordinated germanium [27]. This center gives rise to two luminescence bands associated to triplet-singlet transition — one at 3.1 eV with time constant about 100 μs and another at 4.3 eV due to singlet-singlet transition. The time constant of the UV band is of ~ 5.5 ns at 290 K and ~ 7.5 ns at 10 K [28]. This luminescence is directly related to the oxygen deficiency of silica;

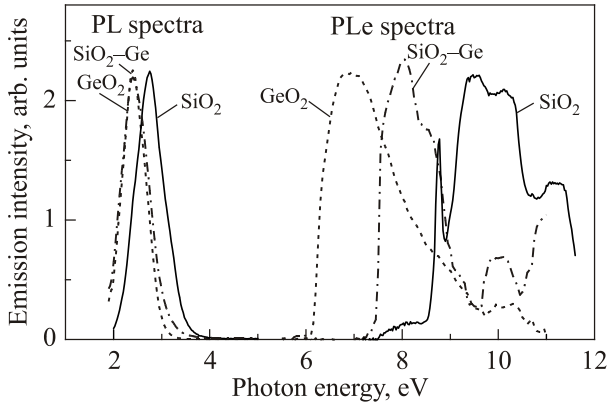

Fig. 16. Photoluminescence (PL) and PL excitation spectra of self-trapped exciton in crystals with α-quartz structure SiO_2, GeO_2 and SiO_2 doped with germanium. T = 80 K.

so, this center is also called a “germanium ODCs” (GeODCs). The luminescence of this center strongly differs from the luminescence related to Ge centers in crystalline quartz.

The nature of luminescence of quartz crystal SiO_2 and GeO_2 as well as SiO_2–Ge is ascribed to creation of self-trapped exciton (STE). Luminescence decay kinetics changes with temperature are presented in Fig. 17. There are two remarkable features. The first peculiarity is the existence of two ranges of thermal quenching at about 130 K and at 180 K, the second peculiarity is observed at low temperature, when single exponential decay turns into two components below 30 K, both components also changing with temperature. There is a remarkably good correspondence between these dependencies for quartz crystal SiO_2 and GeO_2 as well as SiO_2–Ge. These features are explained as zero magnetic field splitting (ZFS) of STE triplet state [29].

The crystal-field, spin-orbit interaction and spin-spin interaction could determine ZFS**.** As the efficiency of the spin-orbit interaction increases rapidly with atomic number, the effect of the interaction should be much larger in GeO_2, than in SiO_2, [30]. For α-quartz the zero-field splitting of the STE is attributed to a strong spin-spin interaction [29]. Similar values of the energy of thermal activation of spin-lattice relaxation, leading to an exchange of population between three levels of the triplet state for STE in GeO_2 and in SiO_2, (and therefore independent of the atomic numbers of Si and Ge) are indicated by the similar values of ZFS in both materials and by the significance of spin-spin interactions in determination of ZFS parameters. On the other hand, whether triplet-singlet transitions are allowed is dependent primarily on spin-orbit interactions. The completely forbidden triplet-singlet transitions become partly allowed only by the mixture with the triplet state with some singlet state by spin-orbit interaction. The influence of spin-spin interaction is not significant for singlet-triplet mixing [31]. The spin-orbit interaction allowing those transitions thus corresponds to the states of oxygen and this is in good agreement with the observation that the decay time constant does not significantly change on moving from Si to Ge. This together with the existence of the two kinds of STE, differing in luminescence polarization with respect to crystal orientation, and thermal activation energy of STE luminescence quenching, are the basis for the STE model, proposed in [32,33], where the exciton self-trapping begins with the occurrence of an electron in an antibonding state leading to weakening of the Si–O bond. Under such conditions, a nonbridging oxygen relaxes in the direction of a bonding oxygen so that the hole of STE is shared with this bonding oxygen. This provides a fixing of STE with O–O bond creation of that NBO of STE with bonding oxygen on the other side of the *c* or *x*, *y* channels. These two cases explain the existence of the two kinds of STE with different energies of thermal quenching and different polarization of luminescence with respect to crystal orientation. The bond strength of the quasi-molecule O–O determines the energy of thermal quenching. Similar model of STE is applied to silica glass. Difference with crystal is manifested through strong inhomogeneous broadening of parameters. Variation of O–O bond of STE determines nonexponential decay of luminescence and specific thermal quenching of intensity. As the result luminescence intensity exponentially grows with cooling [22].

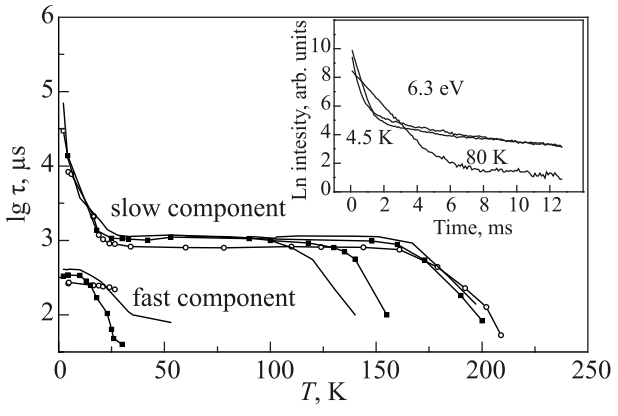

Fig. 17. PL decay kinetics of STE luminescence in GeO_2, SiO_2, SiO_2–Ge crystals with α-quartz structure at different temperatures. lg τ(*T*) of STE in SiO_2 (squares), SiO_2–Ge (line) GeO_2 crystals (circles) with α-quartz structure. Insert — STE PL decay kinetics in GeO_2 crystal.

STE luminescence in glassy GeO_2 is situated at 1.8 eV [34]. It is detected only under x-ray irradiation. Its intensity grows with cooling similarly to silica glass. The background of luminescence related to ODC is obscuring observation of STE in GeO_2 glass, therefore it is not yet studied in the details.

Conclusions

Luminescence of silicon dioxide and germanium dioxide crystal with α-quartz structure or rutile structure was compared with that of oxygen deficient silica and germania glasses. In crystals with α-quartz structure, the luminescence centers similar to ODCs in silica glass are induced by destructive radiation. In germanium dioxide with rutile structure (argutite), the centers exist already after preparation, however in silicon dioxide with rutile structure (stishovite), it is presumed that the centers are excited by “soft” nondestructive x-ray radiation.

Heavily damaged α-quartz is a candidate for oxygen-deficient-center of luminescence analogous to that of silica glass. On the other hand, the induced centers in α-quartz crystal are very similar to the centers observed in a stishovite single crystal. As a result of heavy bombardment, the packing of the α-quartz lattice becomes locally more compact, co-ordination of silicon is changed. Similar defects in stishovite-like clusters are created. Presumably, in

the stishovite structure, such defect is created more easily just by removing an oxygen to an interstitial position. Therefore it is very probable that the defect observed in this work is created in some part by previous ionizing irradiation, when the sample was studied by cathode luminescence and x-ray excited luminescence. On the other hand, stishovite, obtained at high pressure, is metastable and could be transformed into an amorphous state just by heating at 800 K [35].

So, a role of octahedron motifs in constituting ODCs luminescence defects in germania and silica glasses is established.

Acknowledgments

This work is supported by the Latvian Council grant 2013.10–5/014 as well as Latvian National program "IMIS^2".

1. A.N. Trukhin, J.L. Jansons, T.I. Dyuzheva, L.M. Lityagina, and N.A. Bendeliani, *Solid State Commun.* **127**, 415 (2003).
2. A. Paleari, N. Chiodini, D. Di Martino, F. Meinardi, and P. Fumagalli, *Phys. Rev. B* **68**, 184107 (2003).
3. A.N. Trukhin, J.L. Jansons, T.I. Dyuzheva, L.M. Lityagina, and N.A. Bendeliani, *Solid State Commun.* **131**, 1 (2004).
4. A.Trukhin, P. Kulis, J. Jansons, T. Dyuzheva, L. Lityagina and N. Bendeliani, *Phys. Status Solidi* **2**, 584 (2005).
5. A.N. Trukhin, J.L. Jansons, T.I. Dyuzheva, L.M. Lityagina, and N.A. Bendeliani, *J. Phys.: Condens. Matter* **20**, 175206 (2008).
6. K.D. Litasov, H. Kagi, A. Shatskiy, E. Ohtani, D.L. Lakshtanov, J.D. Bass, and E. Ito, *Science Lett.* **262**, 620 (2007).
7. A.N. Trukhin, K. Smits, G. Chikvaidze, T.I. Dyuzheva, and L.M. Lityagina, *Solid State Commun.* **189**, 10 (2014).
8. L.M. Lityagina, T.I. Dyuzheva, N.A. Nikolaev, and N.A. Bendeliani, *J. Crystal Growth* **222**, 627 (2001).
9. T.I. Dyuzheva, L.M. Lityagina, N.A. Bendeliani, and N.A. Nikolaev, *Crystallography (Russia)* **43**, 554 (1998).
10. J.W. Goodrum, *J. Crystal Growth* **13**/**14**, 604 (1972).
11. P. Armand, S. Clement, D. Balitsky, A. Lignie, and P. Papet, *J. Crystal Growth* **316**, 153 (2011).
12. A.N. Trukhin, K. Smits, A. Sharakosky, G. Chikvaidze, T.I. Dyuzheva, and L.M. Lityagina, *J. Luminescence* **131**, 2273 (2011).
13. A.A. Terra, L.J. Borrero-González, L.A.O. Nunes, M.P. Belancon, J.H. Rohling, M.L. Baesso, and O.L. Malta, *J. Appl. Phys.* **110**, 083108 (2011).
14. A.N. Trukhin, *J. Non-Cryst. Solids* **355**, 1013 (2009).
15. A.N. Trukhin, P. Liblik, Ch. Lushchik, and J. Jansons, *J. Luminescence* **109**, 103 (2004).
16. M. Cannas, S. Agnello, F.M. Gelardi, R. Boscaino, A.N. Trukhin, P. Liblik, Ch. Lushchik, M.F. Kink, Y. Maksimov, and R.A. Kink, *J. Phys.: Condens. Matter* **16**, 7931 (2004).
17. M. Cannas, S. Agnello, R. Boscaino, F.M. Gelardi, and A.N. Trukhin, *Phys. Status Solidi C* **4**, 968 (2007).
18. L.N. Skuja, *J. Non-Cryst. Solids* **167**, 229 (1994).
19. L.N. Skuja, *J. Non-Cryst. Solids* **239**, 16 (1998).
20. H. Nishikawa, E. Watanabe, D. Ito, and Y. Ohki, *Phys. Rev. Lett.* **72**, 2101 (1994).
21. R. Boscaino, M. Cannas, F.M. Gelardi, and M. Leone, *Phys. Rev. B* **54**, 6194 (1996).
22. A.N. Trukhin, *Defects in* SiO_2 *and Related Dielectrics*: *Science and Technology*, D. Griscom, G. Pacchioni, and L. Skuja (eds.), Kluwer Academic Publeshers, London (2000), p. 235.
23. M. Stapelbroek and B.D. Evans, *Solid State Commun.* **25**, 959 (1978).
24. A.N. Trukhin and P.A. Kulis, *J. Non-Cryst. Solids* **188**, 125 (1995).
25. L.N. Skuja, *Phys. Status Solidi A* **114**, 731 (1989).
26. A. Trukhin, M. Kink, Y. Maksimov, J. Jansons, and R. Kink, *J. Non-Cryst. Solids* **352**, 160 (2005).
27. L. Skuja, A. Trukhin, and A. Plaudis, *Phys. Status Solidi A* **84**, K153 (1984).
28. M. Leone, S. Agnello, R. Boscaino, M. Cannas, and F.M. Gelardi, *Phys. Rev. B* **60**, 11 (1999).
29. A.N. Trukhin, *Phys. Status Solidi B* **142**, *K* 83 (1987).
30. C. Itoh, K. Tanimura, and A.N. Trukhin, *Nucl. Instr. Meth. Phys. Res. B* **116**, 72 (1996).
31. W. Hayes, M.J. Kane, O. Salminen, R.L. Wood, and S.P. Doherty, *J. Phys. C* **17**, 2943 (1984).
32. A.N. Trukhin, *Fizika Tverdogo Tela* **33**, 1631 (1991).
33. A.N. Trukhin, *Nucl. Instr. Meth. Phys. Res. B* **91**, 334 (1994).
34. A.N. Trukhin, *J. Non-Cryst. Solids* **189**, 291 (1995).
35. S.V. Popova, V.V. Brazhkin, R.N. Voloshin, and M. Grimsdich, *Phys-Usp.* **172**, 486 (2002).